Pis'ma v ZhETF, vol. 99, iss. 12, pp. 789 – 794

Axial anomaly and vector meson dominance model

Ya. Klopot[+1)2)], *A. Oganesian*[+*2)], *O. Teryaev*[+2)]

[+]*Bogoliubov Laboratory of Theoretical Physics, Joint Institute for Nuclear Research, 141980 Dubna, Russia*

[*]*Alikhanov Institute of Theoretical and Experimental Physics, 117218 Moscow, Russia*

Submitted 15 May 2014

A connection between the axial anomaly and the vector meson dominance model is revealed for the processes of pseudoscalar meson-photon transitions. The analytical continuation of the anomaly sum rules, which are exact QCD relations following follow from the dispersive representation of the axial anomaly, to the time-like region is performed. Using these sum rules, the transition form factors of π^0, η, and η' mesons in this region are calculated. A good agreement with the available experimental data is found.

DOI: 10.7868/S0370274X14120029

1. Introduction. One of the cornerstones of hadronic physics is a vector meson dominance model [1]. It may be substantiated by various nonperturbative QCD methods (most recently from AdS/QCD model [2]). In this letter we address yet another connection manifested in the case of meson-photon transition form factors, namely the connection to axial anomaly (supplemented by quark hadron duality).

Axial anomaly [3] is an essential ingredient of any realistic quantum field theory. In particular, the two-photon decay of the pion, $\pi^0 \to \gamma\gamma$, is known to be primarily controlled by the axial anomaly, providing quite an exceptional example of the low-energy process completely determined from the fundamental theory.

It is much less known, that the axial anomaly reveals itself also in the processes, which involve virtual photons. In particular, the photon-meson transitions $\gamma\gamma^* \to M$ (where M is a pseudoscalar meson) can be studied by means of the anomaly sum rules (ASRs), which follow from the dispersive representation of the axial anomaly [4–6]. The ASR approach was applied to π^0, η and η' meson transition form factors (TFFs) in the space-like momentum transfer region ($q^2 < 0$) [7–11].

The pseudoscalar meson TFFs provide an important information about the QCD dynamics, allowing to test our understanding of the low-energy QCD properties as well as perturbative QCD (pQCD) predictions. Recently, the topic of pseudoscalar meson TFFs have gained a significant interest because of unexpectedly large values of the pion TFF at $|q^2| > 10\,\mathrm{GeV}^2$, measured by BABAR Collaboration [12]. These data show an excess over the pQCD predicted limit [13], based on collinear factorization and are hard to explain within the QCD [14, 15]. Although the later data of BELLE Collaboration [16] are quite consistent with the conventional theoretical approach, the controversy remains [17]. The expected high-precision data from BES-III [18, 19], KLOE-2 [20] (in the space-like region, $q^2 < 0$), and CLAS [21, 22] (in the time-like region, $q^2 > 0$) as well as further theoretical investigations (especially those valid in both regions) will give us a more complete understanding of the meson TFFs.

In this work we perform the analytical continuation of the ASRs to the time-like region and also study in detail the small q^2 region, unreachable by the conventional perturbative QCD approach.

2. Axial anomaly: from space-like to time-like region. The vector-vector-axial triangle graph amplitude, where the axial anomaly occurs, contains an axial current $J_{\alpha 5}$ and two electromagnetic currents $J_\mu = \sum_{i=u,d,s} e_i \bar{q}_i \gamma_\mu q_i$ (e_i are quark charges in the units of the absolute value of electron charge),

$$T_{\alpha\mu\nu}(k,q) = \int d^4x d^4y e^{ikx+iqy} \langle 0|T\{J_{\alpha 5}(0) J_\mu(x) J_\nu(y)\}|0\rangle, \quad (1)$$

where k and q are the photons' momenta. In what follows, we limit ourselves to the case when one of the photons is on-shell ($k^2 = 0$).

Considering the unsubtracted dispersion relations, which result in the finite subtraction for the axial current divergence, for the cases of isovector $J^{(3)}_{\alpha 5} = \frac{1}{\sqrt{2}}(\bar{u}\gamma_\alpha\gamma_5 u - \bar{d}\gamma_\alpha\gamma_5 d)$ and octet $J^{(8)}_{\alpha 5} = \frac{1}{\sqrt{6}}(\bar{u}\gamma_\alpha\gamma_5 u +$

[1)] On leave from Bogolyubov Institute for Theoretical Physics, 03680 Kiev, Ukraine.

[2)] e-mail: klopot@theor.jinr.ru; armen@itep.ru; teryaev@theor.jinr.ru

$+ \bar{d}\gamma_\alpha\gamma_5 d - 2\bar{s}\gamma_\alpha\gamma_5 s$) axial currents, one obtains the ASRs [6]:

$$\int_0^\infty A_3^{(a)}(s,q^2;m_i^2)ds = \frac{1}{2\pi}N_c C^{(a)}, \quad a=3,8, \qquad (2)$$

where $N_c = 3$ is a number of colors, $C^{(3)} = \frac{1}{3\sqrt{2}}$, and $C^{(8)} = \frac{1}{3\sqrt{6}}$ are charge factors, m_i are quark masses, and A_3 is the imaginary part of the invariant amplitude at the tensor structure $k_\nu \varepsilon_{\alpha\mu\rho\sigma} k^\rho q^\sigma$ in the variable $(k+q)^2 = s > 0$. The relations (2) are exact: α_s corrections are zero and it is expected that all nonperturbative corrections are absent as well (due to 't Hooft's principle [6, 23]).

Let us stress that ASRs (2) operate with the spectral density of VVA correlator itself and not its divergence. The anomaly here is manifested in the non-additive way, it only fixes the integral of full spectral density of VVA correlator.

As the ASRs (2) do not depend on q^2, they remain valid also in the time-like region ($q^2 > 0$). The explicit way to justify the analytical continuation of ASRs can be demonstrated by the dispersive representation for $A_3(s,q^2)$. Supposing that A_3 decreases fast enough at $|q^2| \to \infty$ and is analytical everywhere except the cut $q^2 \in (0, +\infty)$, it can be expressed as the dispersive integral without subtractions,

$$A_3^{(a)}(s,q^2) = \frac{1}{2\pi}\int_0^\infty dy \frac{\rho^{(a)}(s,y)}{y - q^2 + i\epsilon}, \qquad (3)$$

where $\rho^{(a)} = 2Im_{q^2}A_3^{(a)}$. Then, the ASR (2) for time-like q^2 is given by the double dispersive integral:

$$\int_0^\infty ds \int_0^\infty dy \frac{\rho^{(a)}(s,y)}{y - q^2 + i\epsilon} = N_c C^{(a)}, \; a=3,8. \qquad (4)$$

Note, that generally speaking, the order of integration cannot be interchanged. The real and imaginary parts of the above ASR read:

$$\text{p.v.}\int_0^\infty ds \int_0^\infty dy \frac{\rho^{(a)}(s,y)}{y - q^2} = N_c C^{(a)}, \qquad (5)$$

$$\int_0^\infty ds \rho^{(a)}(s,q^2) = 0, \; a=3,8. \qquad (6)$$

One can easily check, that these sum rules are satisfied in the one-loop massless approximation for the spectral density. For a given flavor i ($i = u,d,s$), it reads [6]:

$$A_3^{(i)} = -\frac{e_i^2 N_c q^2}{2\pi(s-q^2)^2}, \qquad (7)$$

leading to the double spectral density

$$\rho^{(i)}(s,y) = e_i^2 N_c y \delta'(s-y). \qquad (8)$$

Note, that there are no $\mathcal{O}(\alpha_s)$ corrections to the one-loop expression for the spectral density (7) [24].

3. Transition form factors. As we substantiated the validity of the ASRs in the time-like region, it is useful to study their applications. The region close to $q^2 = 0$ is of particular interest for us, as it is hard to reach it by means of perturbative QCD while it is accessible experimentally through Dalitz decays.

3.1. Pion TFF in the time-like region and VMD. Consider the *isovector channel*, i.e., the axial current is $J^{(3)}_{\alpha 5}$. Saturating the lhs of the three-point correlation function (1) with the resonances in the axial channel, singling out the first (pion) contribution and replacing the higher resonances' contributions with the integral of the spectral density, the ASR in the time-like region (5) leads to

$$\pi f_\pi \text{Re}\, F_{\pi\gamma}(q^2) + \int_{s_3}^\infty A_3^{(3)}(s,q^2)ds = \frac{1}{2\pi}N_c C^{(3)}, \qquad (9)$$

where s_3 is the pion duality interval in the isovector channel (which we will fix directly from ASR itself), and the definitions of the meson decay constants f_M^a and TFFs $F_{M\gamma}$ are as follows,

$$\langle 0|J^{(a)}_{\alpha 5}(0)|M(p)\rangle = ip_\alpha f_M^a, \qquad (10)$$

$$\int d^4x e^{ikx}\langle M(p)|T\{J_\mu(x)J_\nu(0)\}|0\rangle = \epsilon_{\mu\nu\rho\sigma}k^\rho q^\sigma F_{M\gamma}. \qquad (11)$$

As the integral of A_3 in Eq. (10) is over the region $s > s_3$, we expect that nonperturbative corrections to A_3 in this region are small enough and we can use the one-loop expression for it.

Then, as $A_3^{(3)} = \frac{1}{\sqrt{2}}(A_3^{(u)} - A_3^{(d)})$, the ASR leads to the pion TFF

$$\text{Re}\, F_{\pi\gamma}(q^2) = \frac{N_c C^{(3)}}{2\pi^2 f_\pi}\left[\text{p.v.}\int_0^{s_3} ds \int_0^\infty dy \frac{\rho^{(a)}(s,y)}{y-q^2}\right] = \frac{1}{2\sqrt{2}\pi^2 f_\pi}\frac{s_3}{s_3 - q^2}. \qquad (12)$$

Here we will make our only assumption, that the duality interval in the axial isovector channel s_3 does not depend on q^2. The numerical value of s_3 was obtained in the limit $-q^2 \to \infty$ of the space-like ASR [7], $s_3 = 4\pi^2 f_\pi^2 \simeq 0.67\,\text{GeV}^2$. This expression coinsides with the one obtained earlier from the two-point correlator analysis [25] and is close to the numerical value obtained from two-point sum rules [26]. In this way we found that the Brodsky–Lepage interpolation formula [27] (which is a one-loop approximation of the ASR) is valid also in time-like region [3)].

[3)] The similarity between Brodsky–Lepage interpolation formula in the space-like region and the vector dominance model in the time-like region is widely known, see, e.g. [28].

We make the key observation that the TFF (12) in the time-like region at $q^2 = s_3$ has a pole, which numerically is close to the ρ-meson mass squared, $m_\rho^2 \simeq$ $\simeq 0.59\,\mathrm{GeV}^2$. Let us stress, that in our approach $m_\rho^2 = m_\omega^2 = s_3$, which can be seen from the expansion of one of the electromagnetic currents in (1) into isovector and isoscalar components provided that the pion duality intervalis universal. This results in the relation between the axial anomaly combined with global quark-hadron duality and VMD in its simplest form when only ρ (and ω) contribute[4)]. Indeed, one can see, that the contributions of the higher mass vector resonances ($m_V^2 > s_3$) are suppressed due to the specific form of the double spectral density (8). As soon as one singles out the pion contribution in the axial channel, the photon is automatically saturated by the ρ-meson only, which is consistent with the VMD model. So, the specific localized form of the anomalous double spectral density (8) provides a foundation for VMD.

Let us note, that from (6) one can also obtain the imaginary part of the pion TFF, $\mathrm{Im}\, F_{\pi\gamma} = \frac{N_c C^a}{2\pi f_\pi}\delta(q^2 - s_3)$, which corresponds to a zero width of the ρ-meson. If we take into account possible small perturbative and nonperturbative corrections and/or use a more sophisticated model of continuum in the axial channel, i.e. substitute the step-function with some regularized (smoothed) one, it will lead to the finite (instead of zero) ρ-meson width in the vector channel. Nevertheless, this variation is significant for $\mathrm{Im}\, F_{\pi\gamma}$ and $\mathrm{Re}\, F_{\pi\gamma}$ only near the pole. That is why, as we are interested in the TFF far from the pole, we can neglect the imaginary part of the TFF. So, in what follows, we suppose $\mathrm{Re}\, F_{M\gamma} = F_{M\gamma}$.

The dispersion relations for the pion TFF revealing connection to VMD model were studied before (see [31] and references therein), but, to our best knowledge without considering the connection to the axial anomaly.

Note also, that the obtained relation for the pion TFF in the time-like region $q^2 > 0$ (12) naturally transforms to the expression for the pion TFF in space-like region $q^2 < 0$, which was obtained in [7]. Therefore, Eq. (12) gives a universal description of the pion TFF at any q^2.

The pole behavior (which corresponds to zero width of the ρ-meson) appeared since we used the one-loop approximation for A_3. Therefore, Eq. (12) can be used not too close to the pole $q^2 = s_3$.

[4)] The dominance of the lower-mass state(s) was pointed out also in holography approach [2] and Padé-approximations analysis [29, 30].

The plot for the pion TFF normalized to its value at $q^2 = 0$, $R_\pi \equiv F_{\pi\gamma}(q^2)/F_{\pi\gamma}(0)$, is shown in Fig. 1. The

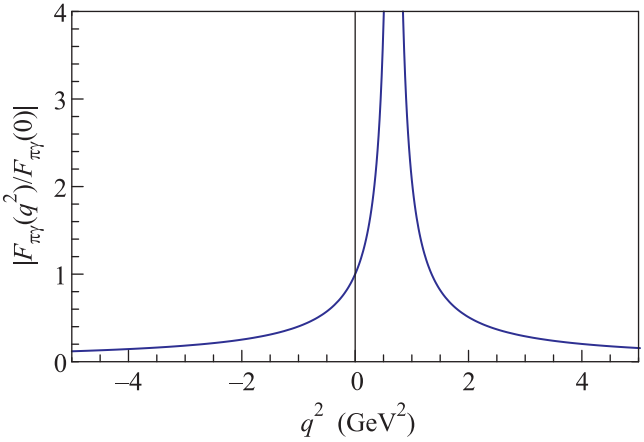

Fig. 1. Pion TFF

dimensionless slope and curvature parameters at $q^2 = 0$, defined for a meson M as $a_M = m_M^2 \partial R_M/\partial q^2|_{q^2=0}$ and $b_M = \frac{1}{2} m_M^4 \partial^2 R_M/\partial (q^2)^2|_{q^2=0}$, are $a_\pi = m_\pi^2/s_3 = 0.027$ and $b_\pi = m_\pi^4/s_3^2 = 0.73 \cdot 10^{-3}$ respectively, which are in agreement with the time-like [32–34] and space-like [28, 35] experimental data. Our result is compatible with the ones obtained in the chiral perturbation theory (ChPT), VMD-based and some other approaches.

3.2. η and η' transition form factors. Let us dwell now on the *octet channel* ($J^{(8)}_{\alpha 5}$) of the ASR. The lowest contributions to the ASR are given by the η- and η'-mesons, both of which should be singled out due to their strong mixing. Then, employing the one-loop expression for the spectral density (7), $A_3^{(8)} = \frac{1}{\sqrt{6}}(A_3^{(u)} + A_3^{(d)} - 2A_3^{(s)})$, the ASR in the time-like ($q^2 > 0$) region leads to

$$f_\eta^8 F_{\eta\gamma}(q^2) + f_{\eta'}^8 F_{\eta'\gamma}(q^2) = \frac{1}{2\sqrt{6}\pi^2}\frac{s_8}{s_8 - q^2}. \qquad (13)$$

The duality interval in the octet channel is determined [8, 10] from the limit $-q^2 \to \infty$ of (13) and the space-like pQCD asymptotes of η, η' TFFs,

$$s_8 = 4\pi^2\{(f_\eta^8)^2 + (f_{\eta'}^8)^2 + 2\sqrt{2}(f_\eta^8 f_\eta^0 + f_{\eta'}^8 f_{\eta'}^0)\}. \quad (14)$$

The Eqs. (13), (14) express the octet combination of the η and η' TFFs in terms of the decay constants f_M^a. For purposes of numerical analysis, we use two sets of the decay constants, obtained in the quark-flavor mixing scheme ([36] and see also [10]):

I) $(f_\eta^8, f_{\eta'}^8, f_\eta^0, f_{\eta'}^0) = (1.38, -0.63, 0.18, 1.35) f_\pi$ (in terms of quark-flavor mixing parameters $f_q = 1.20 f_\pi$, $f_s = 1.65 f_\pi$, $\phi = 38.1^\circ$) [10],

II) $(f_\eta^8, f_{\eta'}^8, f_\eta^0, f_{\eta'}^0) = (1.17, -0.46, 0.19, 1.15) f_\pi$ (in terms of quark-flavor mixing parameters $f_q = 1.07 f_\pi$, $f_s = 1.34 f_\pi$, $\phi = 39.3^\circ$) [36].

The duality interval (14) in terms of quark-flavor mixing scheme parameters reads: $s_8 = (4/3)\pi^2(5f_q^2 - -2f_s^2)$. Numerically, s_8 for the decay constant sets I and II is 0.39 and 0.48 GeV^2 respectively. These numbers, similarly to the isovector channel, are close (with an accuracy of 10–20 %) to the ρ-meson mass squared. The source of the error may be the strange quark mass effect and possible contributions of direct instantons and other non-perturbative effects appearing in the octet channel. Thus VMD-related argument provides an additional (to the discussed in [9]) explanation why the duality interval s_8 is so surprisingly small. Indeed, the similarity of duality intervals in the isovector and octet channels and respective positions of poles in the time-like regions is required for consistency of the anomaly-motivated VMD explanation.

At the same time, the numerical value of the duality interval in the octet channel is determined worse than the one in the isovector channel because of the uncertainty in the decay constants obtained in different analyses. As the ASR can be reliably used in the region sufficiently far away from the pole, this discrepancy is not very important.

From Fig. 2 the reliable region of applicability of Eq. (13) can be estimated as $q^2 \lesssim 0.3\,\text{GeV}^2$ and $q^2 \gtrsim$

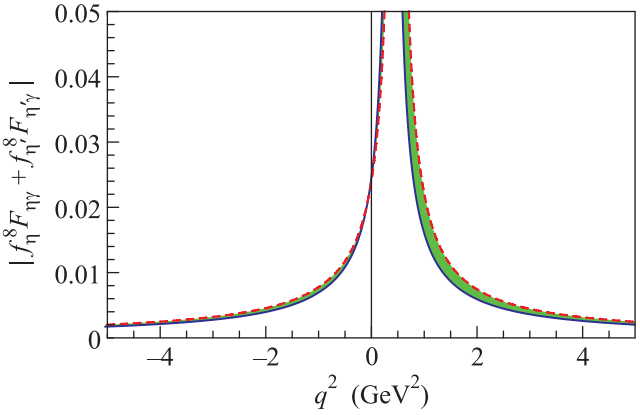

Fig. 2. The octet combination of the TFFs (13)

$\gtrsim 2\,\text{GeV}^2$. The band indicates the region between the lines corresponding to the considered sets (I and II) of decay constants.

In order to obtain the separate expressions for the η and η' TFFs, let us bring another relation [10]. Basing on the widely used hypothesis (see e.g. [37]), that the TFFs of the (unphysical) state $|n\rangle \equiv \frac{1}{\sqrt{2}}(|\bar{u}u\rangle + |\bar{d}d\rangle)$ is related to the pion TFF as $F_{n\gamma}(q^2) = (5/3)F_{\pi\gamma}(q^2)$ (the numerical factor originates from the quark charges $(e_u^2 + e_d^2)/(e_u^2 - e_d^2) = 5/3$), one obtains $\frac{5}{3}F_{\pi\gamma} = = F_{\eta\gamma}\cos\phi + F_{\eta'\gamma}\sin\phi$ (quark-flavor mixing scheme is implied). Combining this equation with (13), (14) and (12), we obtain the η and η' TFFs:

$$F_{\eta\gamma}(q^2) = \frac{5}{12\pi^2 f_s f_\pi}\frac{s_3(\sqrt{2}f_s\cos\phi - f_q\sin\phi)}{s_3 - q^2} + + \frac{1}{4\pi^2 f_s}\frac{s_8\sin\phi}{s_8 - q^2}, \quad (15)$$

$$F_{\eta'\gamma}(q^2) = \frac{5}{12\pi^2 f_s f_\pi}\frac{s_3(\sqrt{2}f_s\sin\phi + f_q\cos\phi)}{s_3 - q^2} - - \frac{1}{4\pi^2 f_s}\frac{s_8\cos\phi}{s_8 - q^2}. \quad (16)$$

In Fig. 3 the plot of the η TFFs (15) (normalized to its value at $q^2 = 0$) is given in the range of

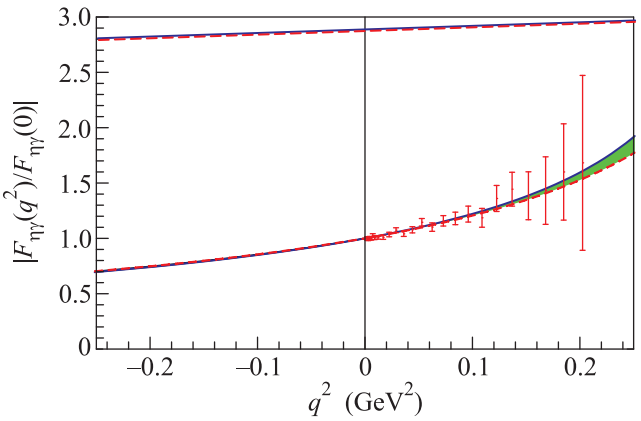

Fig. 3. (Color online) The η meson TFF (15) and A2 Collaboration data [38]

$q^2 \in (-0.25, 0.25)\,\text{GeV}^2$. The blue solid and red dashed curves correspond to the parameter sets I and II respectively, the green band indicates the region between the curves. The data from A2 Collaboration [38] is presented by the red points with error bars. Both decay constants sets (I and II) give $\chi^2/24 = 0.11$. We see a good description of the experimental data. The slope and curvature parameters of the line at $q^2 = 0$ are $a_\eta = 0.54, b_\eta = 0.31$ ($a_\eta = 0.51, b_\eta = 0.27$) for the decay constant set I (II). These numbers are close to the results of [30, 39], ChPT [40], time-like [41], and space-like [28, 35] experimental data fits.

The data of NA60 experiment for the η TFF [41], available in the region of $q^2 \in (0.06, 0.21)\,\text{GeV}^2$ (not shown in Fig. 3), is also in a good agreement with our result (16). Let also note, that the result of NA60 for the $\omega - \pi^0$ time-like TFF (in the process $\omega \to \mu^+\mu^-\pi^0$), where the discrepancy with the VMD model was found, is related to the axial anomaly with two virtual photons, which is beyond the scope of this letter.

In Fig. 4 the plot of the η' TFF (16) (normalized to $F_{\eta'\gamma}(0)$) is given in the range of $q^2 \in (-0.25, 0.25)\,\text{GeV}^2$.

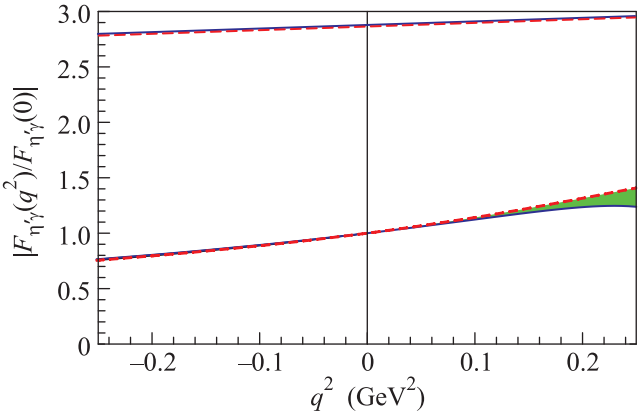

Fig. 4. (Color online) The η'-meson TFF (16)

The blue solid and red dashed curves correspond to the parameter sets I and II respectively. The green band indicates the region between the curves. The slope and curvature parameters of the line at $q^2 = 0$ are $a_\eta = 1.06$, $b_\eta = 0.76$ ($a_\eta = 1.16, b_\eta = 1.19$) for the decay constant set I (II). These numbers are may be compared with [30]: $a_{\eta'} = 1.37(18)$, $b_{\eta'} = 1.94(67)$.

In summary, based on the axial anomaly, we have provided the foundations for the VMD model for the TTFs with one real and one virtual photon. Using the analytical continuation of the ASRs to the time-like region, the TFFs of π^0-, η- and η'-mesons in this region were calculated and compared with the available experimental data.

We would like to thank M. Amaryan, A. Efremov, G. Ecker, E. Kuraev, S. Mikhailov, and N. Stefanis for stimulating discussions and comments. This work is supported in part by RFBR, research projects # 12-02-00613, 12-02-91526, 12-02-00284, 13-02-01060, and Heisenberg–Landau Program (JINR).

1. J. J. Sakurai, Annals Phys. **11**, 1 (1960); R. P. Feynman, *Photon-Hadron Interactions*, Westview Press (1998).
2. H. R. Grigoryan and A. V. Radyushkin, Phys. Rev. D **77**, 115024 (2008).
3. J. S. Bell and R. Jackiw, Nuovo Cim. A **60**, 47 (1969); S. L. Adler, Phys. Rev. **177**, 2426 (1969).
4. A. D. Dolgov and V. I. Zakharov, Nucl. Phys. B **27**, 525 (1971).
5. J. Horejsi, Phys. Rev. D **32**, 1029 (1985).
6. J. Horejsi and O. Teryaev, Z. Phys. C **65**, 691 (1995).
7. Y. N. Klopot, A. G. Oganesian, and O. V. Teryaev, Phys. Lett. B **695**, 130 (2011).
8. Y. N. Klopot, A. G. Oganesian, and O. V. Teryaev, Phys. Rev. D **84**, 051901 (2011).
9. Y. Klopot, A. Oganesian, and O. Teryaev, JETP Lett. **94**, 729 (2011).
10. Y. Klopot, A. Oganesian, and O. Teryaev, Phys. Rev. D **87**, 036013 (2013); arXiv:1211.0874.
11. D. Melikhov and B. Stech, Phys. Lett. B **718**, 488 (2012).
12. B. Auber, Y. Karyotakis, J. P. Leest et al. (BaBar Collaboration), Phys. Rev. D **80**, 052002 (2009).
13. G. P. Lepage and S. J. Brodsky, Phys. Rev. D **22**, 2157 (1980).
14. N. G. Stefanis, A. P. Bakulev, S. V. Mikhailov, and A. V. Pimikov, Phys. Rev. D **87**, 094025 (2013); A. P. Bakulev, S. V. Mikhailov, A. V. Pimikov, and N. G. Stefanis, Phys. Rev. D **86**, 031501 (2012); Acta Phys. Polon. Supp. **6**, 137 (2013).
15. S. S. Agaev, V. M. Braun, N. Offen, and F. A. Porkert, Phys. Rev. D **83**, 054020 (2011).
16. S. Uehara, Y. Watanabe, H. Nakazawa et al. (Belle Collaboration), Phys. Rev. D **86**, 092007 (2012).
17. A. Denig, G. Schott, R. Versaci (BaBar Collaboration), Nucl. Phys. Proc. Suppl. **234**, 283 (2013).
18. D. M. Asner, T. Barnes, J. M. Bian, I. I. Bigi, N. Brambilla, I. R. Boyko, V. Bytev, and K. T. Chao, Int. J. Mod. Phys. A **24**, S1 (2009).
19. M. Unverzagt, J. Phys. Conf. Ser. **349**, 012015 (2012).
20. S. Ivashyn, M. Mascolo, R. Messi, D. Moricciani, A. Nyffeler, G. Venanzoni and KLOE-2 Collaboration, Eur. Phys. J. C **72**, 1917 (2012).
21. M. Amaryan, PoS CD **12**, 061 (2013).
22. *MesonNet 2013 International Workshop Miniproceedings*, ed. by K. Kampf, A. Kupsc, and P. Masjuan, arXiv:1308.2575.
23. G. 't Hooft, in *Recent Developments in Gauge Theories*, ed. by G. 't Hooft et al., Plenum Press, N.Y. (1980).
24. F. Jegerlehner and O. V. Tarasov, Phys. Lett. B **639**, 299 (2006).
25. A. V. Radyushkin, Acta Phys. Polon. B **26**, 2067 (1995).
26. M. A. Shifman, A. I. Vainshtein, and V. I. Zakharov, Nucl. Phys. B **147**, 448 (1979).
27. S. J. Brodsky and G. P. Lepage, Phys. Rev. D **24**, 1808 (1981).
28. H. J. Behrend, L. Criegee, J. H. Field et al. (CELLO Collaboration), Z. Phys. C **49**, 401 (1991).
29. P. Masjuan, Phys. Rev. D **86**, 094021 (2012).
30. R. Escribano, P. Masjuan, and P. Sanchez-Puertas, arXiv:1307.2061.
31. L. G. Landsberg, Phys. Rept. **128**, 301 (1985).
32. R. Meijer Drees, C. Waltham, T. Bernasconi et al. (SINDRUM-I Collaboration), Phys. Rev. D **45**, 1439 (1992).
33. F. Farzanpay, P. Gumplinger, A. Stetz, J. M. Poutissou, I. Blevis, M. Hasinoff, C. J. Virtue, C. E. Waltham, B. C. Robertson, T. Mulera, A. Shor, J. Lowe, and S. H. Chew, Phys. Lett. B **278**, 413 (1992).
34. E. Abouzaid, M. Arenton, A.R. Barker et al. (KTeV Collaboration), Phys. Rev. Lett. **100**, 182001 (2008).

35. J. Gronberg, T.S. Hill, R. Kutschke et al. (CLEO Collaboration), Phys. Rev. D **57**, 33 (1998).
36. T. Feldmann, P. Kroll, and B. Stech, Phys. Rev. D **58**, 114006 (1998).
37. P. del Amo Sanchez, J. P. Lees, V. Poireau et al. (BaBar Collaboration), Phys. Rev. D **84**, 052001 (2011).
38. P. Aguar-Bartolome, J. R. M. Annand, H. J. Arends et al. (A2 Collaboration), arXiv:1309.5648 [hep-ex].
39. C. Hanhart, A. Kupsc, U.-G. Meiβner, F. Stollenwerk, and A. Wirzba, arXiv:1307.5654 [hep-ph].
40. L. Ametller, J. Bijnens, A. Bramon, and F. Cornet, Phys. Rev. D **45**, 986 (1992).
41. R. Arnaldi, K. Banicz, J. Castor et al. (NA60 Collaboration), Phys. Lett. B **677**, 260 (2009).